Available online at www.sciencedirect.com
ScienceDirect
Geochimica et Cosmochimica Acta 74 (2010) 7144–7159
Geochimica et Cosmochimica Acta
www.elsevier.com/locate/gca

A new method integrating high-precision U–Pb geochronology with zircon trace element analysis (U–Pb TIMS-TEA)

B. Schoene [a,b,*], C. Latkoczy [c], U. Schaltegger [a], D. Günther [c]

[a] University of Geneva, Section of Earth Sciences, Geneva, Switzerland
[b] Princeton University, Department of Geosciences, Guyot Hall, Princeton, NJ 08540, USA
[c] ETH Zurich, D-CHAB, Lab of Inorg. Chem., Wolfgang-Pauli-Str. 10, 8093 Zurich, Switzerland

Received 19 March 2010; accepted in revised form 15 September 2010; available online 22 September 2010

Abstract

Increased precision in isotope-dilution thermal ionization mass spectrometry (ID-TIMS) U–Pb geochronology has revealed age complexities in zircon populations that require new tools for understanding how the growth of zircon is related to geologic processes. U and Pb are routinely separated from other elements in dated minerals by ion exchange separation prior to TIMS isotope measurement. We develop a method in which trace elements in the exact same volume of zircon are redissolved and analyzed using solution nebulization inductively coupled plasma sector-field mass spectrometry with matrix-matched external liquid calibration. Using <0.5 ml solution, resulting concentrations are between <1 ppt for elements such as Ti, Nb and Ta and tens of ppb for Zr. By analyzing a series of standard solutions, zircons and procedural blanks, we show that accurate measurements are performed on Zr, Hf, Y, Sc, and the HREE while low-concentration elements can be measured accurately to <5 ppt. We performed combined U–Pb ID-TIMS geochronology with trace element analysis (here called U–Pb TIMS-TEA) on zircons from eight volcanic rocks comprising several volcanic systems and one metamorphic sample. Similar to previous *in situ* trace element analyses, zircon geochemistry is distinct between different samples and records petrogenetic processes such as fractional crystallization, assimilation and/or magma mixing. Unique from *in situ* analysis, U–Pb TIMS-TEA can trace geochemical evolution in accessory minerals with adequate age precision to resolve magmatic processes in rocks at least 200 million years old. This provides a means to identify auto-, ante- and xenocrystic zircon and lead to more robust age interpretations in ID-TIMS U–Pb geochronology. One suite of Cretaceous andesitic zircons shows correlations in geochemistry and absolute time that record evolution of a magmatic system over ~250 ka prior to eruption. Future work will combine U–Pb TIMS-TEA with solution isotopic analysis of Nd, Sr and Hf and will be applied to a host of datable minerals such as monazite, sphene, apatite, rutile, xenotime, and baddeleyite. These combined tools will provide access to an improved understanding of a wide range of igneous and metamorphic processes as a function of time.

1. INTRODUCTION

The integration of geochronological methods with accessory mineral geochemistry has aided in our understanding of how the chemical budgets of igneous and metamorphic systems behave as a function of time and how this reflects large-scale tectonic and thermal processes (e.g. Müller, 2003; Tomaschek et al., 2003; Belousova et al., 2006; Harley et al., 2007). It is now common to characterize internal textures and petrographic context of minerals prior to conducting geochemical microanalysis and/or *in situ* U–Pb dating techniques (ion probe or laser ablation inductively coupled plasma mass spectrometry—LA-ICP-MS) (Griffin et al., 2002; Rubatto, 2002; Kelly and Harley, 2005; Yuan et al., 2008). In geologic environments where the low precision afforded by *in situ* dating is sufficient, this type of work

* Corresponding author at: Princeton University, Department of Geosciences, Guyot Hall, Princeton, NJ 08540, USA. Tel.: +1 609 258 5747.
E-mail address: bschoene@princeton.edu (B. Schoene).

0016-7037/$ - see front matter © 2010 Elsevier Ltd. All rights reserved.
doi:10.1016/j.gca.2010.09.016

provides crucial information for connecting geochronological information with process. However, in many cases it is desirable to have dates for minerals with the highest possible precision because countless geologic processes occur on sub-million year time scales, which becomes irresolvable by *in situ* dating in rocks older than about 20 Ma.

Modern isotope-dilution thermal ionization mass spectrometry (ID-TIMS) U–Pb dating can provide age precision of ⩽0.1% for a single analysis (Ramezani et al., 2007; Schaltegger et al., 2009; Macdonald et al., 2010; Schoene et al., 2010), or ⩽20 ka in rocks ca. 20 Ma. Such high temporal resolution has resulted in complex zircon age populations insisting that in many igneous and metamorphic systems, zircon and other high-U accessory minerals crystallize over a period between 10^4 and 10^6 years, which has also been observed by *in situ* microbeam U–Th–Pb and U-series dating and ID-TIMS dating of <1 Ma volcanic zircons (e.g. Reid et al., 1997; Cooper and Reid, 2003; Turner et al., 2003; Charlier et al., 2005; Simon and Reid, 2005; Tepley et al., 2006; Bachmann et al., 2007, 2010). Interpreting such age spectra is complicated due to the possibility of Pb-loss or mixing between zones of different ages, especially in whole-grain analysis. Alleviating these problems is aided by characterizing dated minerals in terms of their internal textures followed by microsampling in grain-mount prior to TIMS dating (Hawkins and Bowring, 1997; Crowley et al., 2006; Matzel et al., 2006; Schoene and Bowring, 2007).

Detecting and characterizing mineral growth zones and processes would be further improved by knowing the geochemistry of minerals dated by ID-TIMS. This can be partly achieved through characterizing geochemical zonation in minerals *in situ* prior to removing minerals from grain-mount or thin-section and performing ID-TIMS U–Pb geochronology (Corrie and Kohn, 2007; Crowley et al., 2007). The problems with this method are that it is logistically difficult and that geochemistry is measured at the sectioned surface of a mineral while the high-precision U–Pb date represents an average age over the measured volume. Thus, the observed geochemical characteristics are still difficult to relate to the measured date.

In this paper we present a new method that combines the precision of U–Pb ID-TIMS geochronology with trace element analysis (here called U–Pb TIMS-TEA) on the *exact same sample volume used for dating minerals*. This method involves retaining the normally discarded portion of ion exchange chemistry in addition to the U/Pb fraction and analyzing it for trace elements by high-sensitivity solution ICP-MS. As a test of U–Pb TIMS-TEA, we analyze a suite of typical zircons used in ID-TIMS U–Pb zircon geochronology comprising eight volcanic rocks ranging from rhyolitic to basaltic and fragments of one metamorphic zircon megacryst. ID-TIMS U–Pb dates from the same analyzed zircons have been reported elsewhere or presented here. The goal is threefold: (1) to illustrate that zircons originating from a range of magmatic (and metamorphic) compositions can be distinguished geochemically, (2) to confirm that zircon trace elements can record magmatic processes such as assimilation, magma mixing, and fractional crystallization and (3) that zircon geochemistry, when combined with high-precision ages by U–Pb TIMS-TEA, can be used to elucidate processes involved in protracted growth and/or inheritance of zircon in magmatic rocks.

U–Pb TIMS-TEA can also be combined with previously successful methods that measure, for example, Hf and Nd isotopes in zircons or Nd isotopes in sphene in tangent with single-grain ID-TIMS U–Pb dating (Amelin et al., 1999; Amelin, 2004, 2009; Crowley et al., 2006; Schaltegger et al., 2009). Although U–Pb TIMS-TEA is debuted here only in terms of zircon U–Pb geochronology, it can be used to analyze a suite of trace elements on any mineral dated by ID-TIMS, such as monazite, sphene, apatite, rutile, xenotime, baddeleyite, and allanite. Once sample protocol and standardization is established in a laboratory, U–Pb TIMS-TEA can be done with almost no additional effort compared to normal ID-TIMS geochronology yet yields a huge amount of additional geochemical information. It therefore has potential to not only aid in the interpretation of ID-TIMS U–Pb data, but could also provide new insights into the rates of geochemical processes in igneous and metamorphic systems with unprecedented temporal resolution.

2. ANALYTICAL SETUP

ID-TIMS U–Pb geochronology, often called the "gold standard" of geochronology, has been applied to a number of high-U minerals, the most prominent being zircon but including monazite, xenotime, baddeleyite, sphene, apatite, rutile, allanite, and others. It involves the dissolution of multiple-, single-, or partial-grains prior to isotopic analysis by thermal ionization (see Parrish and Noble, 2003). A key step in this process is performing ion exchange separation on the resulting solution to separate U and Pb from other elements in the mineral (Krogh, 1973), which can both inhibit ionization of Pb and U and could cause polyatomic or isobaric interferences. This step is important in thermal ionization mass spectrometry, which provides long-lived stable ion beams and high-sensitivity. Modern low-blank clean air labs, improved tracer solution calibration (Schoene et al., 2006), increased ionization efficiency of U and Pb (Gerstenberger and Haase, 1997), and creative sample preparation and microsampling techniques (e.g. Hawkins and Bowring, 1997; Mundil et al., 2004; Mattinson, 2005; Corrie and Kohn, 2007) have led to remarkable improvements in ID-TIMS geochronology in recent years.

Traditionally, the elements other than U and Pb from a mineral are discarded after ion exchange separation (in the so-called "wash" fraction; Fig. 1). Several studies have successfully measured Hf isotopes in zircon in concert with U–Pb dating, which has yielded valuable information tracing the sources of liquids from which zircon crystallized (Amelin et al., 1999; Crowley et al., 2006; Schaltegger et al., 2009). Here, in addition to retaining the wash fraction from ion exchange chemistry for Hf isotopes, we redissolve this material and introduce it into an inductively coupled plasma (ICP) sector-field (SF) mass spectrometer (MS) for trace element analysis. This section outlines the analytical setup and challenges associated with this type of analysis.

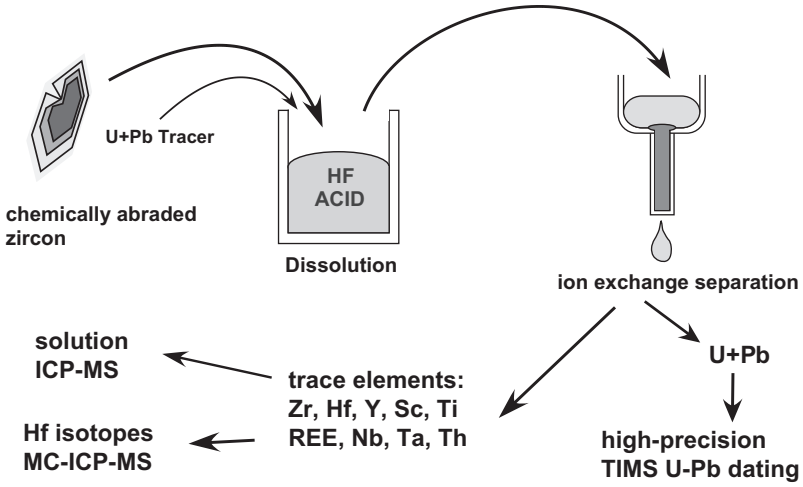

Fig. 1. Cartoon illustrating the U–Pb TIMS-TEA method, adapting traditional zircon dissolution and ion separation procedure with solution ICP-MS trace element analysis.

2.1. ICP-MS calibration standard preparation

Following ion exchange separation, the zircon wash fraction was collected in a small PMP beaker, dried on a hotplate and redissolved in 1 ml of a 0.1 M HF and 0.5 N HNO_3 solution doped with 1 ppb Ir (Fig. 2). This same solution also forms the substrate for a "zircon" external calibration solution, mixed gravimetrically from elemental standards of Zr, Hf, Y, Sc, Nb, Ta, P, U, Th, Pb, Ti and REE in the approximate proportions expected in a real zircon (as determined from a literature survey). The stock calibration solution was diluted into six solutions of differing concentrations with REE ranging from 4 to 750 ppt and Zr from 50 ppb to 10 ppm, and each contained 1 ppb Ir (Fig. 2). The purpose of this is to provide matrix-matched external calibration with internal Ir standardization during ICP-MS measurements. The three calibration solutions of highest concentration were only used for normalization in sample solutions with concentrations above the lower four calibration solutions, which were only reached in several analyses.

2.2. ICP-MS measurement conditions

Isotopes were measured at ETH Zurich by nebulization-based solution analysis using a commercially available ICP-SF-MS instrument (Element2, Thermo Scientific, Bremen, Germany). The instrument is equipped with a compact double-focusing magnetic sector mass separator in reversed Nier–Johnson geometry. Default mass resolution settings of 400, 4000 and 10,000 allowed resolution adjustments to avoid possible spectral interferences. In the configuration used, the instrument was equipped with a microflow PFA nebulizer (PFA-100, Elemental Scientific, Omaha, USA), operated in self-aspirating mode (sample uptake rate = 100 μl/min) and an autosampler for automated

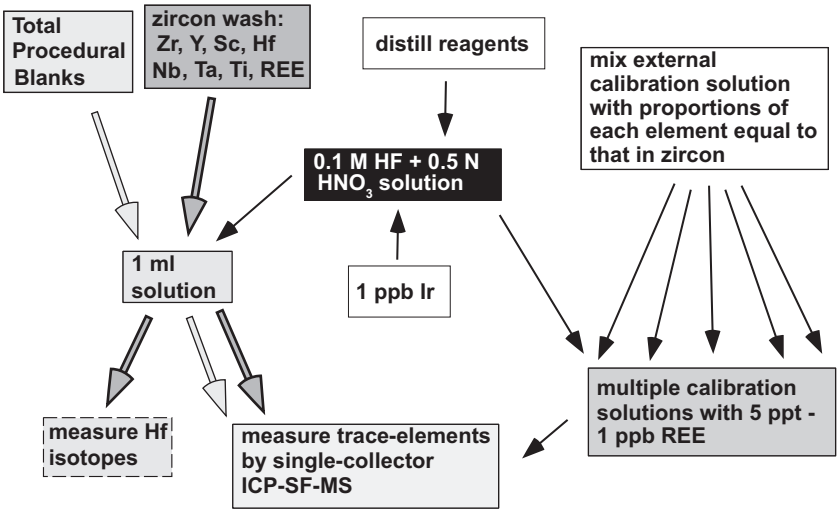

Fig. 2. Flow diagram illustrating the experimental setup for solution nebulization ICP-SF-MS analysis used in this study.

analysis (ASX-100, Cetac, Omaha, USA). Instrumental parameters like rf-power, gas flows and ion lenses were optimized to maximum intensity (1.5×10^6 cps/ppb Ir) together with minimal oxide-formation ($UO^+/U^+ < 4\%$). The set of calibration solutions in addition to a blank solution were measured prior to and during each session; the blank solution was used to flush the transport line in between each sample and was measured every 20 samples. To minimize the effect of plasma fluctuations or different nebulizer aspiration rates between the samples, iridium at 1 ppb final concentration was added to all samples and standards as an internal standard. Concentrations were calculated by least-squares linear interpolation based on normalization with the internal standard, and on calibration curves in the matrix-matched solution described above.

Measurements were carried out in medium mass resolution ($m/\Delta m = 4000$), following a set of experiments to determine whether low- or high-resolution mode was necessary. We found that for the lowest-concentration elements measured, blank levels rather than instrument sensitivity was limiting the precision of the measurements, precluding the usefulness of low-resolution mode. However, many of these elements (e.g. the LREE) were not measurable in high-resolution mode due to low concentrations. A total of about 400 μl of the redissolved zircon wash solutions was used, leaving 600 μl for Hf isotopic analysis on a multi-collector ICP-MS (not presented here).

2.3. ICP-MS blank measurement

In addition to the blank solution (the Ir-doped HF-HNO_3 solution) used to produce external calibration curves, fifteen total procedural blanks were prepared and measured (Electronic annex EA-1). These account for blank introduced by reagents during zircon dissolution and ion exchange chemistry that would not be found in the synthetic Ir-doped HF-HNO_3 solution alone. Procedural blanks were measured along with samples and subject to the calibration curve, identical to samples. An average blank composition, following 2-sigma outlier deletion, was calculated and subtracted from samples. Uncertainties in the blank measurement (2-sigma SD of blank variability, Electronic annex EA-1) were propagated into the uncertainties in sample concentrations.

2.4. Determining zircon trace element concentrations

In order to convert the concentrations within the wash solutions to concentrations in zircon, wash solution elemental concentrations were normalized to $Zr + Hf =$ 497,646 ppm, which is the stoichiometric concentration in the Zr-site of zircon (Hoskin and Schaltegger, 2003). The maximum inaccuracy introduced by this is the total sum of the other elements in the Zr-site, which is $\leqslant 2\%$. Regardless, no uncertainty was propagated in this normalization, as it is a systematic uncertainty and cancels out entirely when taking element ratios. The resulting concentrations, in ppm or permil, are reported for zircons in Electronic annex EA-1. Standard solutions and U/Pb fractions of ion exchange chemistry are reported as concentrations in the solutions analyzed (Electronic annex EA-1).

2.5. U–Pb ID-TIMS analytical techniques

Zircons were separated from bulk samples using standard mineral separation techniques. Individual zircons from each sample were picked for chemical abrasion (Mattinson, 2005) and combined in a quartz beaker for annealing at 900 °C for ~60 h. All grains from a single sample were leached together in 3 ml Savillex beakers in HF + trace HNO_3 for ~12 h at 190 °C, rinsed with water and acetone and then placed in 6 N HCl on a hotplate at ~110 °C overnight. These were then washed several times with water, HCl, and HNO_3. Single grains were then handpicked for dissolution. Each zircon was spiked with ~0.004 g of the EARTHTIME ^{202}Pb–^{205}Pb–^{233}U–^{235}U (ET2535) tracer solution. $^{235}U/^{205}Pb = 100.20$ was used for the ET2535 tracer, and no uncertainty in tracer calibration was propagated for the purposes of this study. Zircons were not weighed prior to dissolution, so estimating U and Pb concentrations (as ppm) was not possible. Zircons were dissolved in ~70 μl 40% HF and trace HNO_3 in 200 μl Savillex capsules at 210 °C for 48+ h, dried down and redissolved in 6 N HCl overnight. Samples were then dried down and redissolved in 3 N HCl and put through a modified single 50 μl anion exchange column (Krogh, 1973). U and Pb were collected in the same beaker and dried down with a drop of 0.05 M H_3PO_4 and analyzed on a single outgassed Re filament in a Si-gel emitter, modified from Gerstenberger and Haase (1997). Measurements were performed on a Thermo Scientific Triton thermal ionization mass spectrometer at the University of Geneva.

Pb was measured in dynamic mode on a modified Masscom secondary electron multiplier (SEM). Deadtime for the SEM was determined by periodic measurement of NBS-982 for up to 1.3 Mcps and observed to be constant at 23.5 ns. Multiplier linearity was monitored every few days between 1.3×10^6 and <100 cps by a combination of measurements of NBS-981, -982 and -983, and observed to be constant if the Faraday to SEM yield was kept between ~93% and 94% by adjusting SEM voltage. Baseline measurements were made at masses 203.5 and 204.5 and the average was subtracted from each peak after beam decay correction. Interferences on ^{202}Pb and ^{205}Pb were monitored by measuring masses 201 and 203 and also by monitoring masses 202 and 205 in unspiked samples, and no corrections were applied. Pb fractionation was determined by use of the ^{202}Pb–^{205}Pb double spike with a $^{202}Pb/^{205}Pb$ of 0.99989.

U was measured in static mode on Faraday cups and 10^{12} ohm resistors as UO_2^+. Oxygen isotopic composition was monitored by measurement of mass 272 on large U500 loads (Wasserburg et al., 1981), yielding an average value of ~0.00205. Baselines were measured at ±0.5 mass units for 30 s every 50 ratios. Correction for mass-fractionation for U was done with the double spike assuming a sample $^{238}U/^{235}U$ ratio of 137.88. The composition used for the ET2535 tracer is the same as that reported in Schoene et al. (2010).

All common Pb was assigned to blank, whose composition was measured at UNIGE over the course of this study as total procedural blanks. After 2-sigma outlier rejection, the tracer-subtracted composition of fifteen blanks was: $^{206}Pb/^{204}Pb = 18.08 \pm 0.66$, $^{207}Pb/^{204}Pb = 15.79 \pm 0.45$, $^{208}Pb/^{204}Pb = 37.55 \pm 0.93$ (2-sigma standard deviations). Measured ratios were reduced using the algorithms of Schmitz and Schoene (2007) and Crowley et al. (2007). ^{230}Th disequilibrium was corrected using an ad-hoc $Th/U_{magma} = 4 \pm 1$.

3. RESULTS

Because the U–Pb TIMS-TEA method had never been conducted previously, we initially had two primary concerns that could potentially limit the accuracy of this method: (1) whether elements were fractionated during ion exchange separation; in other words, does Sc/Y in the measured zircon wash solution equal Sc/Y in the zircon? (2) How accurate are the measurements in terms of blank subtraction, matrix-matching, and instrument sensitivity? To test these concerns, we passed 15 variable sized aliquots of the calibration solution (equivalent to <1 ppm REE in a zircon to >100 ppm REE in a zircon) through ion exchange chemistry to evaluate elemental fractionation. Results are presented in Electronic annex EA-1, where "w" at the end of the sample name refers to the wash solution, "U.Pb" refers to the U + Pb fraction, and "all" refers to minerals that were not passed through ion exchange chemistry. Those without these terms after the sample name are wash solutions. We also dissolved and analyzed the ca. 337 Ma Plesovice zircon, whose trace elements have been well-characterized by laser ablation ICP-MS in Slama et al. (2008). This standard is in fact not homogeneous with respect to trace element concentrations, but has a reproducible and unique REE pattern with depleted HREE, which is ideal for testing REE measurements. Large fragments of this standard were dissolved and analyzed with and without passing them through ion exchange chemistry.

Finally, we applied this method to a suite of unknown zircons typical of those used in high-precision ID-TIMS U–Pb dating.

3.1. Standard solution measurements

Passing the standard solution through ion exchange chemistry is useful for testing both the magnitude of elemental fractionation and also the accuracy of the resulting elemental ratios. After ion exchange separation, the resulting solutions contained between <1 and 600 ppt REE, which is similar to those in the zircon wash solutions. Fig. 3 shows the measured ratios of Sm/Nd and Ce/Nd as a function of concentration. For all concentrations, the measured ratio was within the uncertainty of the true value of 1 (as stated by the vendor of the REE standard), but the uncertainty becomes very large (>100%) below ~5–10 ppt (Fig. 3). This is a result of both the analytical uncertainty in measuring smaller quantities and also the effect of error magnification in blank subtraction. Other element ratios, such as Y/Sc and Zr/Hf, are also very reproducible (Fig. 3). However, there is a systematic offset of Zr/Hf for [Zr] > 1000 ppb when using the low-concentration calibration solution, which is corrected when using the calibration solution of matched concentrations. Zircon samples with similarly high concentrations were therefore calibrated using similar concentration solutions. Overall, our results indicate that if uncertainties are calculated correctly, the accuracy of the results is not jeopardized. In general uncertainties in measurements and blank subtraction were a function of the concentration: 50+ ppt = ±2–4%; 10–50 ppt = ±5–10%; <5 ppt = 50–100+%.

3.2. Standard zircon measurements

We analyzed six fragments of Plesovice zircon that were not passed through column chemistry and measured both the U–Pb and wash fractions from 12 grains that had passed through columns. Our aliquot of Plesovice was the same used for ID-TIMS U–Pb geochronology from the University of Geneva and the Massachusetts Institute of Technology in Slama et al. (2008). Though the trace elements in Plesovice show large variations, zirconium-normalized results for all 18 grains agree well with the range of element concentrations measured in that study by LA-ICP-MS. Our concentrations (Zr normalized) for Hf are 9000–12,000 ppm and Slama et al. (2008) report 8000–14,000 ppm. Both studies measure 300–800 ppm Y.

Measurement of the U/Pb fraction of these zircons reveals that for all elements except Nb and Ta, $\ll$1% of the total elemental budget was found in the U/Pb fraction. This high degree of accuracy of calculated ratios is further enhanced because there is a linear correlation between, for example, Y(wash)/Y(U/Pb) and Zr(wash)/Zr(U/Pb), so the Zr-normalized concentrations are even less affected by column fractionation (Fig. 4). Further work is needed to determine whether Nb and Ta are found in the U or Pb portion of column chemistry and whether this can be remediated in future work (by modifying the column chemistry). Furthermore, P was entirely lost during the procedure, despite high concentrations of P found in other studies (see summary in Hoskin and Schaltegger, 2003).

All 18 of our measurements have REE patterns that also agree well with those reported in Slama et al. (2008), which have depleted HREE. Relatively low Gd/Yb has been observed previously in metamorphic zircons that grew in the presence of garnet (Rubatto, 2002; Kelly and Harley, 2005)(Fig. 5).

3.3. TIMS-TEA on zircon unknowns

To illustrate the applicability of U–Pb TIMS-TEA to zircons typically used for ID-TIMS dating, we present data from a suite of zircons that crystallized in magmas ranging from basaltic to rhyolitic and compare those results to metamorphic trace element signatures of Plesovice (Electronic annex EA-1). Each of these are from single zircons subjected to the normal ID-TIMS geochronology procedure outlined in Section 2.5 (see also Schoene et al., 2010), except for metamorphic Plesovice zircons, which were fragments of large crystals and were dated at ca.

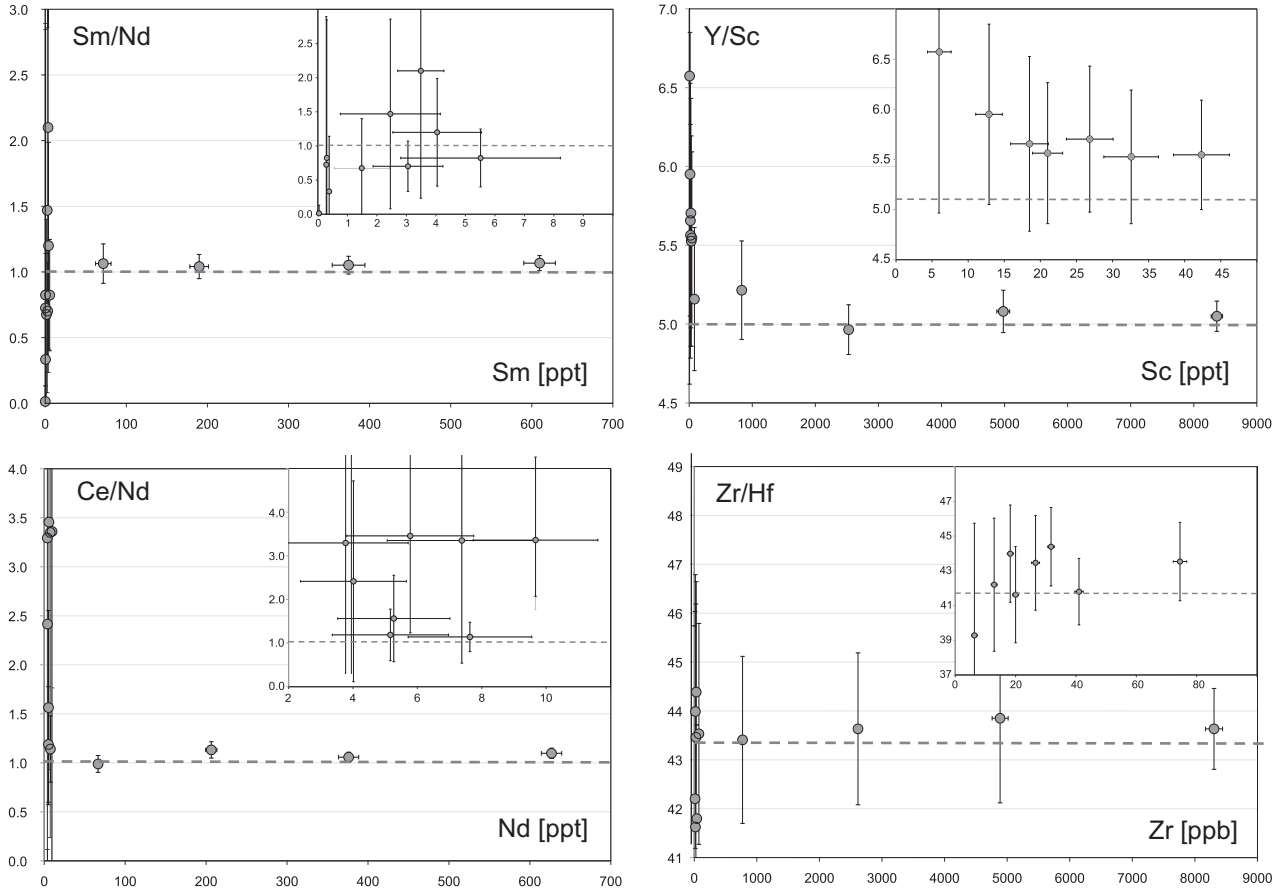

Fig. 3. ICP-MS data for the wash fractions of mixed "zircon" standard solutions of known composition that were put through ion exchange separation to simulate the zircon procedure and check for elemental fractionation. The horizontal dashed line indicates the true value, determined by gravimetric mixing of commercially available elemental standards. Insets show the same data with different scale, emphasizing the low-concentration data. Note that though the data become imprecise at low concentrations, they remain accurate within reported uncertainties.

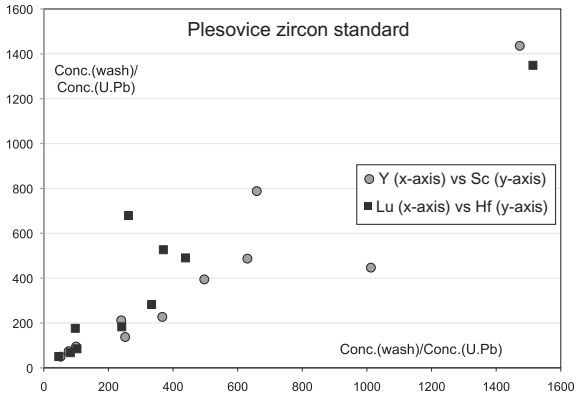

Fig. 4. Plots indicating the concentration ratio of an element in the wash fraction (Conc.(wash)) over that in the U–Pb fraction (Conc.(U.Pb)) for the Plesovice standard. A ratio of ~100 indicates that 1% of the element was left in the U/Pb fraction during ion exchange chemistry, thus introducing a 1% inaccuracy in calculated concentrations in zircon. Note the high degree of covariance between different elements (positive slope of the curves), indicating that ratios of elements are more accurate than concentrations of single elements.

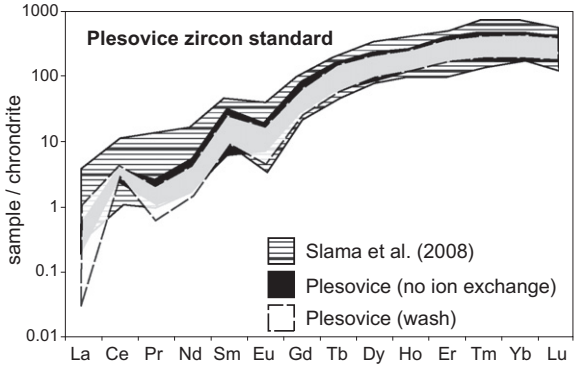

Fig. 5. Rare-earth element spider diagrams for Plesovice zircon. Data are plotted from wash fractions ($n = 12$), and from grains not put through ion exchange separation ($n = 6$), in order to evaluate whether the chemical separation fractionates elements and whether the stoichiometric Zr-normalization is accurate. Data from Slama et al. (2008), determined by LA-ICP-MS are also shown for comparison. Data are normalized to Zr + Hf = 497,646 ppm in single grains and all data are normalized to chondrite values of Sun and McDonough (1989). Note the excellent agreement between all three data sets.

337 Ma on separate fragments prior to this study (Slama et al., 2008).

U–Pb isotopic data from NMB03-1, NYC-N10, and LM4-100 are published in Schoene et al. (2010). NMB03-1 is an example of a felsic segregation within the North Mountain Basalt, the lowermost flow of the ca. 201 Ma Central Atlantic Magmatic Province in the Bay of Fundy, Canada (Schoene et al., 2006, 2010). Samples NYC-N10 and LM4-100 are thin (several cm thick) rhyolitic ash beds from near the ca. 201 Ma Triassic–Jurassic boundary, sampled from the New York Canyon, Nevada, USA, and the Utcubamba valley, northern Peru, respectively (Schoene et al., 2010).

Samples CD07-1, 08CD-4, 08CD-6, and 08CD-10 come from the early Cretaceous Dabeigou Group, Chengde Basin, North China. CD07-1 is an andesitic tuff from within a thick clastic sedimentary sequence. The 08CD samples are older andesitic flows from within the same section, with relative age relations as follows: 08CD-4 > 08CD-6 > 08CD-10. U–Pb isotopic data for the 08CD samples are reported in Table 1.

Analyzed zircons were measured for Zr, Hf, the REE, Y, Sc, Th, Nb, Ta, P, and Ti. As mentioned previously, P was absent in the solutions, suggesting it was lost during dissolution and/or ion exchange procedures, though the reason for this is not yet known. Ti was generally <3 ppt in the analyzed solutions, which was similar to blank levels, and so we are hesitant to attach significance to these data and do not report them in Electronic annex EA-1. Nb, Ta, La, and Pr concentrations are similarly low in many samples, but easily measured in others; these elements are reported in Electronic annex EA-1.

While a full petrogenetic analysis of the zircon trace element characteristics is beyond the scope of this study, here we highlight some of the key points that illustrate the potential of TIMS-TEA to achieve the goals outlined in Section 1. REE patterns from zircons from the North Mountain Basalt (NMB03-1) show higher REE concentrations but shallower HREE (lower Yb/Gd) compared to zircons from a felsic ignimbrite (NYC-N10) (Fig. 6). Nearly all zircons have positive Ce anomalies (Ce/Ce*) and negative Eu anomalies (Eu/Eu*), which is a function of fluid oxidation state, and plagioclase fractionation, respectively, and is discussed in detail elsewhere (Hinton and Upton, 1991; Belousova et al., 2002, 2006; Hoskin and Schaltegger, 2003). North Mountain Basalt zircons have very negative Eu anomalies (Fig. 6). Two of the NYC-N10 zircons have LREE patterns with La > Nd (Fig. 6), which is also seen in several zircons we measured from other samples, and this will be discussed below. Because La and Pr are often near blank levels, the accuracy of quantitatively evaluating Ce/Ce* must be evaluated on each sample individually and is not explored in detail here.

Trace element correlation diagrams (Fig. 7) reveal that zircon from different rocks have markedly different trace element characteristics. Plots of Th/U vs. Y/Sc, Yb/Gd vs. Eu/Eu*, Y/Hf vs. Lu/Sc, and Y/Hf vs. Sc/Th are shown in Fig. 7. The metamorphic Plesovice zircon and the North Mountain Basalt zircons fall well outside the fields all the other magmatic zircons. The rhyolitic to andesitic zircons either fall into distinct clusters that typify zircons from each sample (e.g. Yb/Gd vs. Eu/Eu*), or fall onto trends with partial to no overlap (e.g. Y/Hf vs. Lu/Sc and Y/Hf vs. Sc/Th). The significance of these observations will be discussed in Section 4.2.

Fig. 8 plots $^{206}Pb/^{238}U$ date vs. Y/Hf and Sc/Th for zircons from the ca. 201 Ma samples (NMB03-1, LM4-100, NYC-N10) and the early Cretaceous andesites (08CD-4, 08CD-6, 08CD-10). The three ca. 201 Ma samples, though having very different Y/Hf and Sc/Th from sample to sample, do not show any trends in time. The ca. 128 Ma andesitic zircons, however, show a trend of decreasing Y/Hf and increasing Sc/Th over ~250 ka. Other trace elements ratios show similar characteristics to those in Fig. 8.

4. DISCUSSION

4.1. The importance of mineral inclusions in zircon trace elements

Previous attempts to measure zircon trace elements following dissolution have received scrutiny because of the possibility of mineral inclusions and/or altered zones controlling the trace element budget of zircon (see Hinton and Upton, 1991; Hoskin and Schaltegger, 2003). Microinclusions of, for example, monazite, plagioclase, sphene or apatite could cause distinct REE patterns in the host zircon, most notably manifested as LREE and/or MREE enrichment (see Bea and Montero (1999) and Prowatke and Klemme (2005) for examples of REE patterns from these minerals). Several analyses from NYC-N10 zircons (Fig. 6b) show modestly elevated LREE that could possibly be inclusion-related. Only one analysis from our study shows highly elevated LREE (08CD-4 z6, Electronic annex EA-1). However, similar patterns were measured in zircons originating from differentiated magmatic rocks by LA-ICP-MS, and these were attributed to host melt chemistry (Belousova et al., 2006). Whitehouse and Kamber (2002) also observe significant LREE enrichments in SIMS analyses of Archean zircons, and discount inclusions as a viable source for this. They noted that inclusions of monazite or apatite would carry other traceable signatures, such as elevated Th/U or Sr. Though we did not measure Sr, in no case are elevated LREE associated with elevated Th/U or noticeably older $^{206}Pb/^{238}U$ dates (e.g. >1 Ma), which might also be expected from monazite inclusions (e.g. Parrish, 1990). Other anomalous chemical signatures such as elevated Y from xenotime or major elements in garnet, plagioclase, K-feldspar, or melt inclusions, may be expected if contamination by inclusions were a problem. It should be noted also that elevated levels of Al, Fe, and Ca have been attributed to low-temperature incorporation by metamict and/or recrystallized zircon (Geisler and Schleicher, 2000; Belousova et al., 2002; Geisler et al., 2003). Our initial attempts to measure major elements (Ca, Al, Mg, Na and Fe; not shown here) were at blank levels and were not pursued further given limited amount of solution and the desire to increase count rates on important elements.

We therefore attribute the trace element abundances measured in this study to melt/mineral partitioning in

Table 1
U–Pb isotopic data.

Sample (a)	Radiogenic isotope ratios												Isotopic ages					
	Th/U (b)	Pb*/Pb$_c$ (c)	Pb$_c$ (pg) (c)	^{206}Pb/^{204}Pb (d)	^{208}Pb/^{206}Pb (e)	^{207}Pb/^{206}Pb (e)	% Err (f)	^{207}Pb/^{235}U (e)	% Err (f)	^{206}Pb/^{238}U (e)	% Err (f)	Corr. coef.	^{207}Pb/^{206}Pb (g)	± (f)	^{207}Pb/^{235}U (g)	± (f)	^{206}Pb/^{238}U (g)	± (f)
08CD-4																		
z5	1.14	24	1.00	1229	0.366	0.048805	0.323	0.135075	0.344	0.020073	0.035	0.627	138.46	7.58	128.65	0.42	128.12	0.04
z6	1.25	27	1.12	1386	0.400	0.048708	0.277	0.134730	0.296	0.020062	0.038	0.542	133.78	6.51	128.34	0.36	128.05	0.05
z7	1.52	9	0.68	426	0.485	0.048649	0.995	0.134474	1.057	0.020048	0.076	0.827	130.93	23.40	128.11	1.27	127.96	0.10
z8	1.00	31	1.13	1669	0.318	0.048644	0.232	0.134609	0.249	0.020070	0.039	0.494	130.69	5.45	128.23	0.30	128.10	0.05
08CD-6																		
z5	1.12	23	1.42	1212	0.358	0.048808	0.313	0.135036	0.335	0.020066	0.047	0.523	138.61	7.36	128.61	0.40	128.07	0.06
z6	1.07	27	1.27	1433	0.342	0.048756	0.271	0.134762	0.289	0.020047	0.037	0.550	136.10	6.36	128.37	0.35	127.95	0.05
z7	0.94	48	1.07	2591	0.302	0.048644	0.150	0.134398	0.171	0.020038	0.066	0.503	130.72	3.52	128.04	0.21	127.90	0.08
z8	1.08	30	1.63	1565	0.346	0.048605	0.248	0.134510	0.269	0.020071	0.058	0.454	128.83	5.83	128.14	0.32	128.10	0.07
08CD-10																		
z5	1.02	49	1.70	2586	0.326	0.048651	0.148	0.134590	0.161	0.020064	0.037	0.453	131.05	3.49	128.21	0.19	128.06	0.05
z6	1.03	36	1.14	1893	0.329	0.048712	0.201	0.134770	0.216	0.020066	0.039	0.472	133.99	4.72	128.38	0.26	128.07	0.05

(a) z1, z2, etc. are labels for fractions composed of single zircon grains or fragments; all fractions annealed and chemically abraded.
(b) Model Th/U ratio calculated from radiogenic ^{208}Pb/^{206}Pb ratio an iterated with ^{206}Pb/^{238}U age.
(c) Pb* and Pb$_c$ represent radiogenic and common Pb, respectively; mol% ^{206}Pb* with respect to radiogenic, blank and initial common Pb.
(d) Measured ratio corrected for spike and fractionation only. Mass-fractionation was corrected using the EARTHTIME ^{202}Pb–^{205}Pb tracer (Schoene et al., 2010).
(e) Corrected for fractionation, spike, and common Pb; all common Pb assumed to be blank: ^{206}Pb/^{204}Pb = 18.39 ± 1.2%; ^{207}Pb/^{204}Pb = 15.45 ± 1.3%; ^{208}Pb/^{204}Pb = 37.62 ± 1.6% (all uncertainties 2SD). ^{206}Pb/^{238}U and ^{207}Pb/^{206}Pb ratios corrected for initial disequilibrium in ^{230}Th/^{238}U using Th/U [magma] = 4 ± 1.
(f) Errors are 2-sigma, propagated using the algorithms of Schmitz and Schoene (2007) and Crowley et al. (2007).
(g) Calculations are based on the decay constants of Jaffey et al. (1971). ^{206}Pb/^{238}U and ^{207}Pb/^{206}Pb ages corrected for initial disequilibrium in ^{230}Th/^{238}U using Th/U [magma] = 4 ± 1.

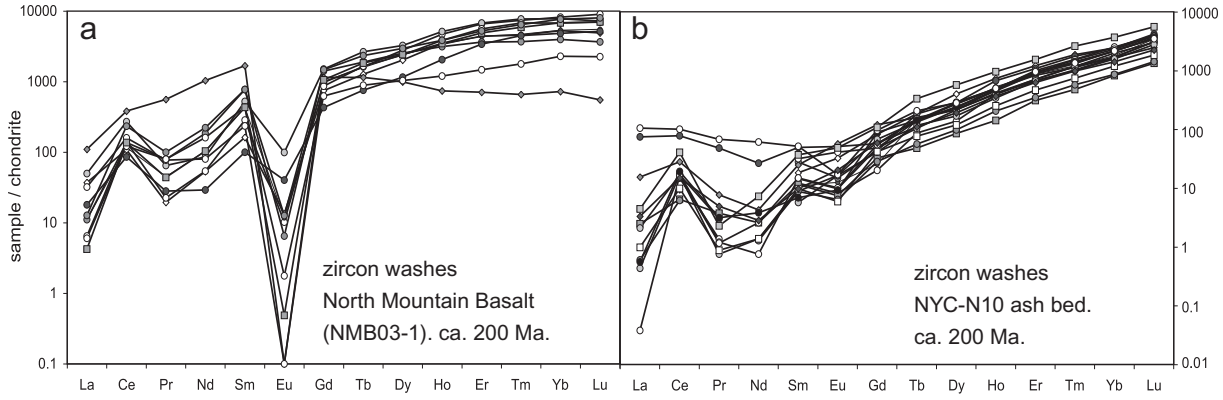

Fig. 6. REE patterns of zircons used in ID-TIMS geochronology and analyzed for trace elements by U–Pb TIMS-TEA. (a) Zircons from NMB03-1, a ca. 201.4 Ma pegmatitic segregation of the North Mountain Basalt, Nova Scotia, and (b) zircons from ca. 201.4 Ma volcanic ash bed from the New York Canyon, Nevada. U–Pb data published in Schoene et al. (2010). All data normalized to 497,646 ppm Zr + Hf in zircon and also to the chondrite composition of Sun and McDonough (1989). See text for discussion.

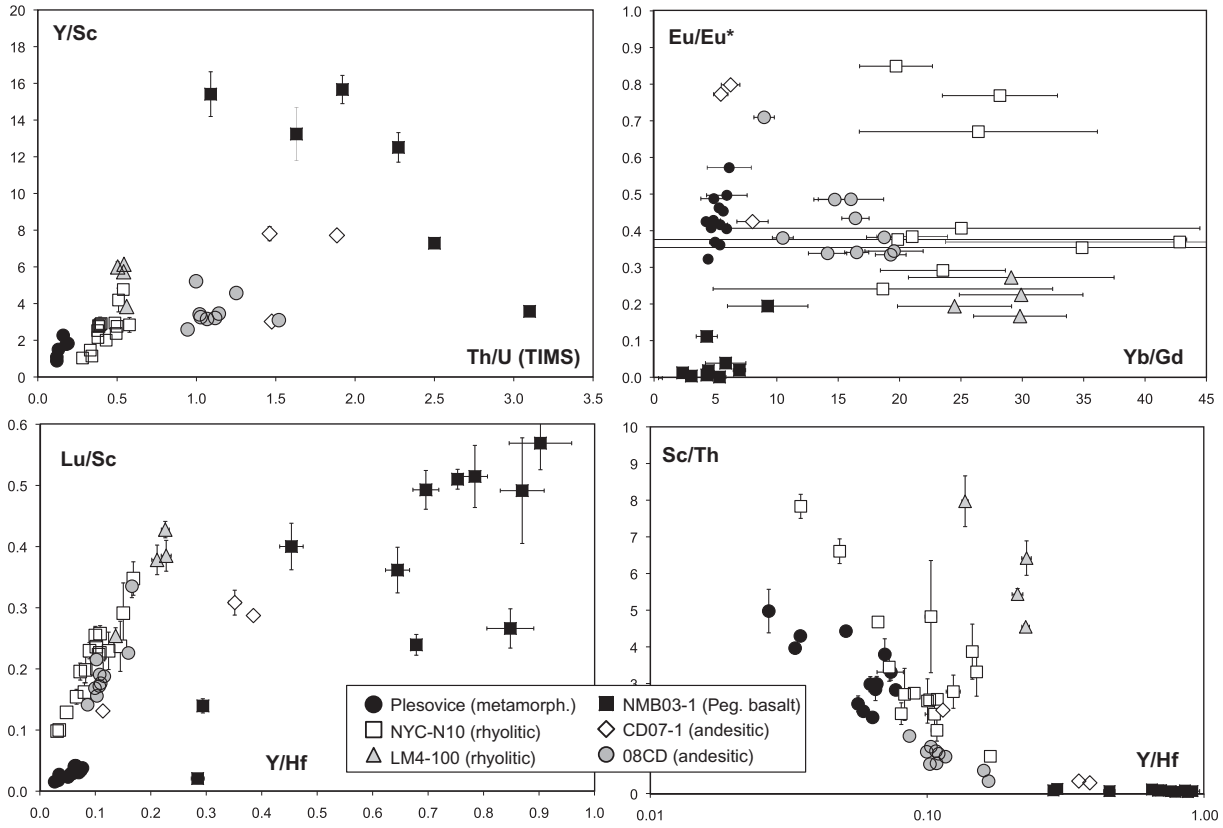

Fig. 7. Trace element correlation diagrams for zircon washes from metamorphic and volcanic zircons determined using the U–Pb TIMS-TEA method. Different samples form distinct groups and/or trends, interpreted to reflect differences in geochemical composition of the liquid from which they crystallized. Eu/Eu* is the europium anomaly, calculated as [Eu]/sqrt([Sm]*[Gd]) using concentrations already normalized to chondrite. Th/U (TIMS) is the Th/U calculated using the the $^{206}Pb/^{238}U$ date and $^{206}Pb/^{208}Pb$ determined by ID-TIMS and assuming concordance between the U–Pb and Th–Pb isotopic systems.

zircon rather than inclusions or late-stage recrystallization, though pursuing reliable methods for monitoring the importance of inclusions should be done in future work. The problem of inclusions is certainly avoided in part by analyzing single-grains handpicked to be free of inclusions, as is standard in ID-TIMS U–Pb geochronology. Additionally, the ubiquitous use of the chemical abrasion technique (Mattinson, 2005) during zircon preparation not only dissolves metamict portions of zircon with Pb-loss and/or recrystallization, but also can dissolve melt inclusions and some important soluble minerals such as monazite, xenotime and apatite.

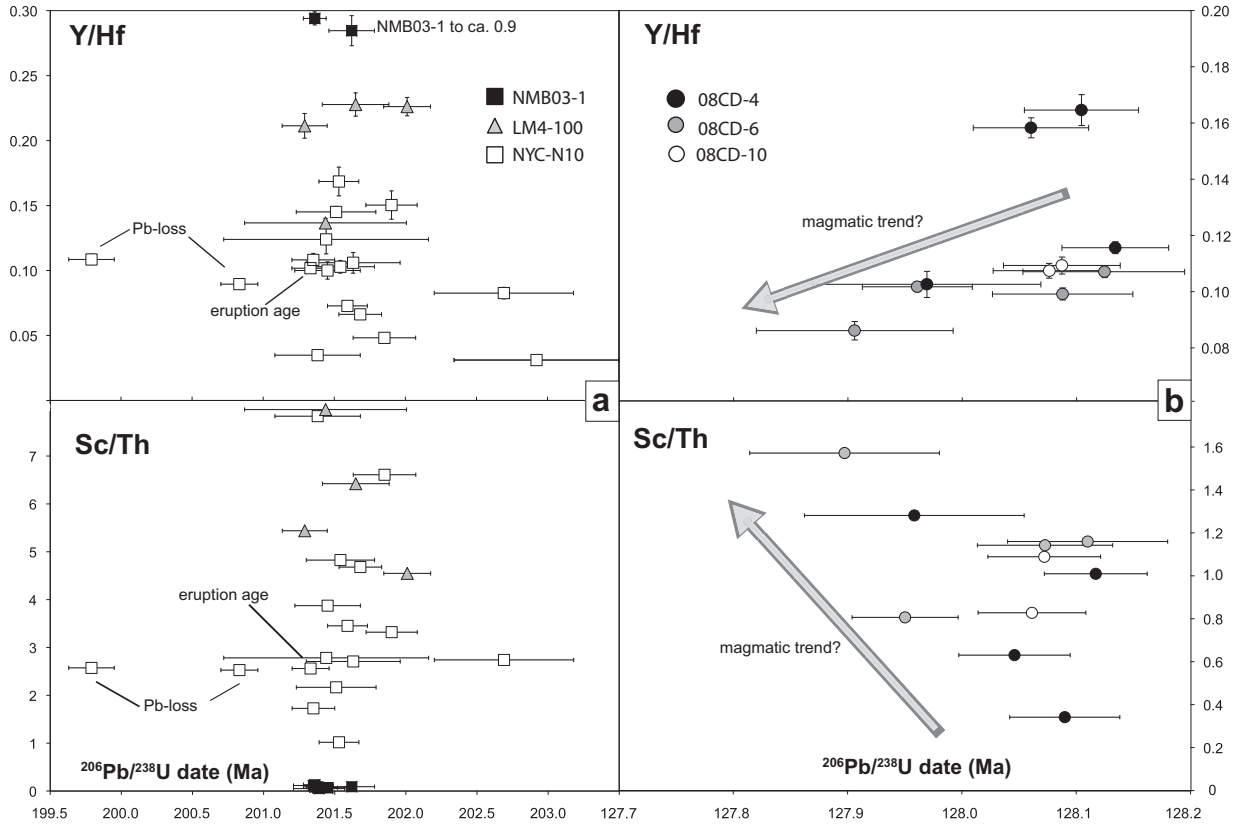

Fig. 8. Application of the U–Pb TIMS-TEA method: zircon trace elements as a function of high-precision time. (a) Y/Hf and Sc/Th for zircons from two ash beds and the North Mountain Basalt, near the Triassic–Jurassic boundary (U–Pb data are in Schoene et al., 2010). Discussion of interpretations (Pb-loss vs. eruption age) is given in Schoene et al. (2010). Note there is no correlation in NYC-N10 trace elements as a function of time, indicating these zircons did not likely form in a closed magmatic system, but instead are composed of auto-, ante-, and xenocrystic grains. (b) Zircons from sequential andesitic flows in China (U–Pb isotopic data is in Table 1) do show a trend of Y/Hf and Sc/Th with time, possibly recording pre-eruption magma differentiation. Such data can be used to interpret eruption ages vs. Pb-loss or inheritance.

4.2. U–Pb TIMS-TEA on zircon unknowns

Our initial results allow us to address the goals set out in Section 1: (1) to illustrate that zircons originating from a range of magmatic (and metamorphic) compositions can be distinguished geochemically; (2) to confirm that zircon trace elements can record magmatic processes such as assimilation, magma mixing, and fractional crystallization and (3) that zircon geochemistry, when combined with high-precision ages, can be used to elucidate processes involved in protracted growth and/or inheritance of zircon in magmatic rocks.

4.2.1. Do zircon trace elements distinguish magmatic source?

Compilation of data from eight rocks reveals that zircon from different samples, in some cases of similar magma composition (e.g. rhyolitic), have distinct trace element signatures (Fig. 7). Our analyses reproduce the rare-earth patterns typical of zircon: LREE poor, HREE rich, with distinct positive Ce and negative Eu anomalies (Ce/Ce* and Eu/Eu*; Fig. 6) (e.g. Hanchar et al., 2001; Hinton and Upton, 1991; Hoskin and Ireland, 2000; Hoskin et al., 2000; Sano et al., 2002; Thomas et al., 2002). More importantly is that small variations in REE patterns distinguish zircons from different samples, such as Eu/Eu* (an indicator of plagioclase fractionation) vs. Yb/Gd (sensitive to fractionation of amphibole, pyroxene or garnet), shown in Fig. 7. Though some previous workers (e.g. Hoskin et al., 2000) suggest that zircon REE patterns are not useful as petrogenetic indicators, our work and that of Belousova et al. (2002) show that although zircon REE are broadly similar regardless of magma composition, subtle differences in the slope of the HREE, Eu/Eu* and Ce/Ce* can be used to distinguish zircons from different sources. In fact, basaltic, andesitic, and rhyolitic zircon from different samples tend to fall on similar areas of the trace element correlation diagrams (Fig. 7), consistent with the observations of Belousova et al. (2002). However, given the overlap of many of the zircon samples, we refrain from suggesting that trace element characteristics alone could be used to determine major element composition of the source magma (i.e. rhyolitic vs. basaltic). Therefore, zircon trace elements could not necessarily be used to blindly determine zircon provenance or parental liquid in detrital zircon studies, as discussed in some trace element in zircon studies (Hoskin and Ireland, 2000; Wilde et al., 2001; Cavosie et al., 2004; see also

discussion below on partition coefficient uncertainties). This, however, is not the goal of U–Pb TIMS-TEA given that ID-TIMS geochronology is not the proper tool for detrital zircon studies. Our contribution here is aimed at examining small differences in trace elements as a function of a highly resolved times-series for samples that are relatively well-characterized geologically.

TIMS-TEA could therefore be useful in routine ID-TIMS U–Pb geochronology for assessing the influence of xeno- and antecrystic zircon on age populations—a practice typically done by optical inspection of zircon and evaluation of age spreads in concordia space (e.g. Ramezani et al., 2007; Davydov et al., 2010; Schoene et al., 2010). Additionally, identification of metamorphic vs. igneous minerals, which is often guided in U–Pb dating by the Th/U ratio or grain morphology (e.g. Rowley et al., 1997; Aleinikoff et al., 2002), can be enhanced with additional geochemical information provided by TIMS-TEA. For example the metamorphic Plesovice standard zircon has low Th/U and Y/Sc compared to magmatic zircon (Fig. 7), the latter being consistent with it having grown in the presence of garnet. Mineral trace elements have proven useful in distinguishing metamorphic vs. igneous growth by *in situ* characterization (e.g. Schaltegger et al., 1999; Rubatto, 2002; Kelly and Harley, 2005), but this has never before been directly accessible to ID-TIMS dating.

4.2.2. Do zircon trace elements record magma evolution?

The fact that zircon from different samples in this study are often distinguishable from one another in trace element correlation diagrams suggests their composition represents different geochemistry of the liquids they crystallized in. Therefore, the within-sample trends observed in these diagrams suggest that the liquid compositions are changing in time or space during zircon crystallization. In the case of the igneous zircons (all but the Plesovice zircon), their trace element ratios can change either because the chemistry of the liquid is changing, because partition coefficients (D_i) in zircon are changing as a function of pressure, temperature or major element composition in the magma (e.g. Si content), or due to non-equilibrium partitioning. These options are explored below.

Fine scale oscillatory zonation in zircon has been long recognized both optically and by cathodoluminescence and backscatter electron imaging (e.g. Hanchar and Miller, 1993; Vavra et al., 1996, 1999; Corfu et al., 2003). The cause of zoning is clearly chemical in origin, though how it forms is still poorly understood. Hofmann et al. (2009) used NanoSIMS to show that fluctuations in trace element ratios (by up to a factor of three) occur in zircon on the sub-micron scale and at least roughly correlate with larger-scale zoning observed by cathodoluminescence. Their preferred hypothesis for its formation calls for disequilibrium partitioning at the crystal surface (i.e. trapping of elements on the zircon surface), which is perhaps affected by slow-diffusing elements at the crystal–melt interface. If disequilibrium partitioning is important on larger spatial scales, inferences made about magmatic processes based on trace element data may be jeopardized. More systematic studies are needed to test, for example, if disequilibrium effects on the micron scale are averaged out over larger spatial scales such that trends across zircon grains still preserve evolving magma composition. Indeed, the broad consistency of zircon/melt D_i values measured for the REE in natural systems (Hinton and Upton, 1991; Sano et al., 2002; Thomas et al., 2002) and determined experimentally (Watson, 1980; Rubatto and Hermann, 2007; Luo and Ayers, 2009) suggest that equilibrium partitioning plays a large role in the uptake of trace elements into zircon. It is worth noting, though, that the most widely adopted partitioning estimates (Sano et al., 2002; Thomas et al., 2002) still differ by a factor of 2–3 for some MREE and HREE, and by orders of magnitude for the LREE (see summary in Hanchar and van Westrenen, 2007).

Two recent studies explore temperature and pressure effects of zircon D_i values, and these could help explain differences between published partition coefficient datasets (Rubatto and Hermann, 2007; Luo and Ayers, 2009). The experiments of Rubatto and Hermann (2007) show about an order of magnitude decrease in D_i values for the REE with 250 °C increase in temperature. However, partition coefficients for trace element *ratios* do not vary by more than a factor of two over 250 °C (e.g. Y/Hf in zircon at 800 °C relative to Y/Hf in zircon at 1050 °C, given constant Y/Hf in the melt), and do not correlate well with temperature. Thus, one can argue that systematic changes in trace element ratios in zircon probably reflect changes in magma chemistry rather than temperature. Given the paucity of partitioning data for zircon (and other accessory minerals) with respect to temperature, pressure, and major element composition of the magma, more work is warranted.

Though uncertainties in partition coefficients hinder our ability to calculate melt compositions from zircon trace elements, inferences on magmatic process can still be drawn from mineral trace element compositions resolved in relative or absolute time. Reid et al. (in press), employing serial sectioning combined with SIMS trace element analysis, use decreasing Zr/Hf in zircon as an indicator of progressive zircon crystallization in the Bishop Tuff magmatic system (e.g. measuring core to rim; see also Claiborne et al., 2007). They also observed concomitant trends in Eu/Eu* and Nd/Yb which they attribute to melt evolution, consistent with other geologic constraints on melt evolution for the Bishop Tuff. Griffin et al. (2002) and Belousova et al. (2006) use combined Hf isotope and Y/Hf data from zircon to evaluate melt evolution and zircon sources—this is a powerful approach because Hf isotopes are not affected by changing partition coefficients. They show that zircon trace elements and isotopes, when combined with petrology of host rocks, are robust recorders of magma evolution. Several other studies also argue that zircon trace elements record magma trace element composition rather than (or in addition to) changing temperature, pressure, or disequilibrium effects (e.g. Ballard et al., 2002; Miller and Wooden, 2004; Claiborne et al., 2007, 2010; Miller et al., 2007).

Our own data plotted on trace element correlation diagrams are consistent with magma differentiation, mixing and/or assimilation playing a role in zircon trace elements. The most notable example is the North Mountain Basalt

zircons, which crystallized from a residual liquid derived from extensive eutectic basalt crystallization (Greenough and Dostal, 1992). The highly negative Eu/Eu* can be explained easily by high degrees plagioclase fractionation (Fig. 7), whereas the depleted HREE (low Yb/Gd) may derive from the garnet bearing source of the basaltic parent liquid.

Perhaps more important are the trends in trace element ratios observed within single samples. For example, each sample shows an increase in Y/Hf with increasing Lu/Sc (Fig. 7), though each sample has different endpoints and different slopes for the trends. Samples NYC-N10, LM4-100 and the 08CD samples have overlapping but slightly different evolution lines. Though a more detailed petrologic examination of each sample would be required to identify the origins of each evolution path (e.g. if certain minerals fractionated from the magma to cause the observed trends), these systematic correlations suggest that zircon trace elements in different samples evolved through similar petrogenetic processes but from different parental magmas. A similar conclusion can be drawn from Y/Hf vs. Sc/Th, which shows negative, non-overlapping trends for each sample. Some samples have trace element ratios that change by factors of 6–8—well above those observed in experiments (Rubatto and Hermann, 2007) or hypothesized to be from disequilibrium crystallization (Hofmann et al., 2009). Thus, there is strong evidence that trace elements in zircon measured by U–Pb TIMS-TEA are indicative of magmatic processes. While this method lacks the ability to resolve trace element evolution transects that is possible using *in situ* analysis, it has the advantage of providing information about geochemical evolution of magmas or metamorphic fluids in *absolute* time. Thus, using both methods on the same zircon populations may be enlightening.

4.2.3. A new tool: zircon trace elements with high-precision time

U–Pb isotopic data have been published by Schoene et al. (2010) for samples LM4-100, NMB03-1, and NYC-N10, which are volcanic rocks from near the ca. 201 Ma Triassic–Jurassic boundary. $^{206}Pb/^{238}U$ dates for zircons from ash bed sample NYC-N10 show age variability over >1 Ma (with <200 ka uncertainty on individual points), leading Schoene et al. (2010) to the conclusion that the zircons represent a complex mixture of xeno-, ante-, and autocrystic zircons (i.e. ranging from inherited to those crystallized shortly before eruption; Miller et al., 2007). We have used U–Pb TIMS-TEA to determine complementary geochemistry for the exact same zircons in order to explore the geochemical evolution of the magmatic system with time (Fig. 8a). In the previous section, we argued that the marked trends in trace element correlation diagrams between different samples formed through magmatic processes affecting distinct parental magmas (Fig. 7). However, there is no obvious correlation with time for any trace element patterns in the Triassic–Jurassic samples (Y/Hf and Sc/Th with time are shown in Fig. 8a). This observation, combined with those trends in Fig. 7, leads to the hypothesis that the zircons were a mix of grains picked up from different magma batches either at depth or during the eruption and deposition of the ash bed. In such a scenario, these zircons may be considered antecrystic, given they came from different magma batches having evolved from the same parental magma. Such evidence supports the notion that determining eruption ages from zircon populations must be done with care, especially with regard to weighted-mean dates. Zircons from the North Mountain Basalt, which form a single population with a weighted-mean $^{206}Pb/^{238}U$ date of 201.38 ± 0.02 Ma (MSWD = 1.1; Schoene et al., 2010), also show large variations in trace element correlation diagrams. A strong negative correlation in Y/Hf vs. Sc/Th (Fig. 7) shows that they may be related by a continuous magmatic processes, but that it happened in <50–100 ka, consistent with field and petrologic evidence suggesting the residual melt that crystallized the zircons formed *in situ*, and post-eruption (Greenough and Dostal, 1992).

As a complementary example, three Cretaceous andesites from China, which fall in close stratigraphic succession and within the same short-duration magnetic reversal, contain zircons that show trace element variation as a function of time (Fig. 8b and Table 1). These same zircons fall on the same magmatic trends in trace element correlation diagrams such as Y/Hf vs. Lu/Sc and Y/Hf vs. Sc/Th (Fig. 7). It is important to note the apparent mafic to felsic evolution followed by the entire suite of zircons in this study: higher Y/Hf and lower Sc/Th correspond to zircons originating in more mafic magmas (Fig. 7). One could thus argue that the trends in time shown by the 08CD zircons reflect a differentiation trend within a magmatic system. It follows that zircons with the lowest Y/Hf and highest Sc/Th from each sample represent crystallization in more differentiated magma and these youngest grains best approximate the eruption age of the flow(s). The older grains corresponding to higher Y/Hf and lower Sc/Th represent crystallization during magma differentiation prior to eruption. Note that the trend in trace element chemistry also argues against Pb-loss as a possible cause of the ca. 250 ka spread in dates, which could be an important constraint provided by U–Pb TIMS-TEA in future geochronologic studies.

4.3. Applications and future improvements

Modern ID-TIMS U–Pb geochronology can detect single- to sub-grain age differences to ⩽0.1% of the age, illustrating that in rocks <100 Ma U–Pb TIMS-TEA can trace the geochemistry of systems at timescales of ⩽100 ka. The examples shown above (Figs. 7 and 8) indicate that zircon trace elements can be a useful tool in interpreting zircon populations with complex age distributions in terms of growth and Pb-loss. In fact, in some cases U–Pb TIMS-TEA could be used to screen for Pb-loss by tracking trace element evolution patterns. As such, we anticipate this method will open new doors for understanding the rates of magmatic and metamorphic processes, especially given that most of these processes occur on timescales that are currently not resolvable using *in situ* dating techniques in rocks older than several million years.

TIMS-TEA will also provide a new means for combining *in situ* and ID-TIMS dating and geochemical analysis to optimize the benefits of each tool. Because the spatial resolution of ID-TIMS geochronology is largely limited to fragments of minerals tens of microns in size, this technique inevitably averages both age and trace elements over a relatively large volume of material compared to *in situ* microanalysis techniques. Ages are weighted towards high-U and/or large volume zones and trace elements by TIMS-TEA are weighted towards high concentration and/or large volume zones. Analyzing trace elements *in situ* prior to TIMS-TEA will lead to a better understanding of any potential decoupling of age and trace element patterns measured by U–Pb TIMS-TEA.

Though this initial work highlights zircon trace elements, U–Pb TIMS-TEA can be applied to any mineral that is datable by ID-TIMS, such as monazite, sphene, apatite, rutile, allanite, xenotime, etc. Different ICP-MS protocols will need to be developed for each mineral, given the different trace element compositions. Similarly, ion exchange separation for these minerals can be more complicated than for zircon, so testing the importance of trace element fractionation will be necessary. Alternatively, samples could be aliquoted prior to ion separation if the amount of radiogenic Pb in the U–Pb fraction is not restrictive. Aliquoting is certainly necessary in order to measure Hf, Nd, or Sr isotopes in the wash fractions of various geochronometers (as has been accomplished with Nd and Hf isotopes for zircon in tangent with ID-TIMS geochronology; Amelin et al., 1999; Amelin, 2004; Crowley et al., 2006; Schaltegger et al., 2009). Because allanite, monazite, sphene, apatite and xenotime have abundant LREE, U and Pb, aliquoting the solution prior to or after ion separation will be possible to measure Hf and Nd (and Sr for apatite) by TIMS or MC-ICP-MS. In young samples, isotope dilution for determining tracer isotope compositions will not be necessary, especially since low precision parent/daughter elemental ratios will be measured by solution ICP-MS during TIMS-TEA. In older samples, isotope dilution may be required for simultaneous determination of Nd and Hf isotopes, though Amelin et al. (1999, 2004) and Amelin (2009) show that this is possible at the single mineral scale using a variety of sequences for spiking and conducting ion separation chemistry.

Another potentially powerful application of U–Pb TIMS-TEA involves combining it with mineral-trace element thermometers, such as the Ti-in-zircon thermometer (Watson et al., 2007). We found that precision greatly suffers in samples with <5 ppt in the analyzed solution, which prevented useful measurements of Ti. The limits of detection on the Element2 ICP-MS are lower, so identifying and eliminating sources of trace element contaminants will be important in future work. Better ionization or slower sample uptake during analysis would also decrease the amount of solution needed, enabling for higher sensitivity. Given these potential improvements, we hope to apply this tool to a wider range of trace elements in zircon, such as P, Ba, Nb, Ta, Mn in addition to Ti and other major elements. Given the potential importance of Ti-in-zircon thermometry for understanding the thermal conditions of zircon growth (Watson et al., 2007), targeting Ti will be an important future improvement. Success would enable the resolution of geochemistry, temperature, and sub-permil time constraints in geologic environments for the first time.

5. SUMMARY AND CONCLUSIONS

We present a new method that utilizes the residual liquid from routine ion exchange separation employed during ID-TIMS U–Pb geochronology in order to characterize trace elements in the analyzed material. The so-called U–Pb TIMS-TEA method benefits from the fact that the trace elements and high-precision date come from the exact same volume of material, holding a key advantage to analyzing trace elements *in situ* followed by removing grains from epoxy mounts and performing ID-TIMS U–Pb analysis on grain fragments. Combining these two approaches may be ideal.

The dissolved zircons were dated by ID-TIMS and measured by ICP-SF-MS to levels as low as several ppt. We found that currently, analytical blank is the primary limiting factor in low-concentration analyses, and suggest means to ameliorate this problem.

Analysis of standard solutions subjected to the zircon sample preparation procedure, in addition to standard zircons with known trace element characteristics, yield accurate results whose precision on concentration varies between $\leqslant$2% for high concentrations (>50 ppt) and >50% for very low concentrations (<5 ppt).

Elemental fractionation during ion exchange chemistry is less than analytical uncertainty. As analytical uncertainty is improved, samples with adequate Pb and U for ID-TIMS analysis could be aliquoted prior to ion exchange chemistry to avoid related uncertainties, especially for more complicated chemical separation procedures commonly used on sphene, apatite, rutile, allanite, etc.

Application to a suite of zircons realistically used in high-precision dating studies has been successful and yields comparable trace element signatures and trends to previous work characterizing variation in zircon. These results show geochemical trends within single samples and wide variation between different samples and rock compositions.

Two case studies are presented, one that shows within a suite of volcanic zircons with a resolvable spread in U–Pb dates, a lack of coinciding evolution in trace elements suggests the presence of xeno- and antecrysts within the ash bed. The other example presents a sequence of three Cretaceous andesitic flows that contain zircons showing trace element evolution over ~250 ka, suggesting the observed spread in zircon dates results from magma differentiation prior to eruption, rather than Pb-loss or inheritance from country rock.

Future work will involve applying this method to a wider range of minerals and elements and testing its utility to a plethora of geologic environments. Combining high-precision age with tracer isotopes (Nd, Hf, and Sr), and trace elements used for thermometry (e.g. Ti-in-zircon, Zr-in-rutile, and Zr-in-sphene; Hayden and Watson, 2007; Watson et al., 2007) could provide new constraints on the temperature-geochemical-time evolution of geologic systems.

ACKNOWLEDGMENTS

This manuscript benefited greatly from reviews by D. Davis, J. Hanchar, and the associate editor Y. Amelin. Andesitic zircon samples from the Chengde Basin were kindly provided by H. He. M. Chiaradia, M. Ovtcharova, and M. Senn provided analytical assistance at the University of Geneva. Research was funded by the Fonds National de Recherche Scientifique of Switzerland.

APPENDIX A. SUPPLEMENTARY DATA

Supplementary data associated with this article can be found, in the online version, at doi:10.1016/j.gca.2010.09.016.

REFERENCES

Aleinikoff J. N., Wintsch R. P., Fanning C. M. and Dorais M. J. (2002) U–Pb geochronology of zircon and polygenetic titanite from the Glastonbury Complex, Connecticut, USA: an integrated SEM, EMPA, TIMS, and SHRIMP study. *Chem. Geol.* **188**, 125–147.

Amelin Y. (2004) Sm–Nd systematics of zircon. *Chem. Geol.* **211**, 375–387.

Amelin Y. (2009) Sm–Nd and U–Pb systematics of single titanite grains. *Chem. Geol.* **261**, 53–61.

Amelin Y., Lee D.-C., Halliday A. N. and Pidgeon R. T. (1999) Nature of the Earth's earliest crust from hafnium isotopes in single detrital zircons. *Nature* **399**, 252–255.

Bachmann O., Charlier B. L. A. and Lowenstern J. B. (2007) Zircon crystallization and recycling in the magma chamber of the rhyolitic Kos Plateau Tuff (Aegean arc). *Geology* **35**, 73–76.

Bachmann O., Schoene B., Schnyder C. and Spikings R. (2010) The $^{40}Ar/^{39}Ar$ and U/Pb dating of young rhyolites in the Kos-Nisyros volcanic complex, Eastern Aegean Arc, Greece: age discordance due to excess 40Ar in biotite. *Geochem. Geophys. Geosyst.* **11**, Q0AA08. doi:10.1029/2010gc003073.

Ballard J., Palin M. and Campbell I. (2002) Relative oxidation states of magmas inferred from Ce(IV)/Ce(III) in zircon: application to porphyry copper deposits of northern Chile. *Contrib. Mineral. Petrol.* **144**, 347–364.

Bea F. and Montero P. (1999) Behavior of accessory phases and redistribution of Zr, REE, Y, Th, and U during metamorphism and partial melting of metapelites in the lower crust: an example from the Kinzigite Formation of Ivrea-Verbano, NW, Italy. *Geochim. Cosmochim. Acta* **63**, 1133–1153.

Belousova E. A., Griffin W. L., O'Reilly S. Y. and Fisher N. I. (2002) Igneous zircon: trace element composition as an indicator of source rock type. *Contrib. Mineral. Petrol.* **143**, 602–622.

Belousova E. A., Griffin W. L. and O'Reilly S. Y. (2006) Zircon crystal morphology, trace element signatures and Hf isotope composition as a tool for petrogenetic modelling: examples from eastern Australian granitoids. *J. Petrol.* **47**, 329–353.

Cavosie A. J., Wilde S. A., Liu D., Weiblen P. W. and Valley J. W. (2004) Internal zoning and U–Th–Pb chemistry of Jack Hills detrital zircons: a mineral record of early Archean to Mesoproterozoic (4348–1576 Ma) magmatism. *Precambrian Res.* **135**, 251–279.

Charlier B. L. A. et al. (2005) Magma generation at a large hyperactive silicic volcano (Taupo, New Zealand) revealed by U–Th and U–Pb systematics in zircons. *J. Petrol.* **46**, 3–32.

Claiborne L. L., Miller C. F., Walker B. A., Wooden J. L., Mazdab F. K. and Bea F. (2007) Tracking magmatic processes through Zr/Hf ratios in rocks and Hf and Ti zoning in zircons: an example from the Spirit Mountain batholith, Nevada. *Mineral. Mag.* **70**, 517–543.

Claiborne L., Miller C. and Wooden J. (2010) Trace element composition of igneous zircon: a thermal and compositional record of the accumulation and evolution of a large silicic batholith, Spirit Mountain, Nevada. *Contrib. Mineral. Petrol.* **160**, 511–531.

Cooper K. M. and Reid M. R. (2003) Re-examination of crystal ages in recent Mount St. Helens lavas: implications for magma reservoir processes. *Earth Planet. Sci. Lett.* **213**, 149–167.

Corfu F., Hanchar J. M., Hoskin P. W. O. and Kinny P. (2003) Atlas of zircon textures. In *Zircon*, vol. 53 (eds. J. M. Hanchar and P. W. O. Hoskin). Mineralogical Society of America, Washington, DC, pp. 468–500.

Corrie S. L. and Kohn M. J. (2007) Resolving the timing of orogenesis in the Western Blue Ridge, southern Appalachians, via in situ ID-TIMS monazite geochronology. *Geology* **35**, 627–630.

Crowley J. L., Schmitz M. D., Bowring S. A., Williams M. L. and Karlstrom K. E. (2006) U–Pb and Hf isotopic analysis of zircon in lower crustal xenoliths from the Navajo volcanic field: 1.4 Ga mafic magmatism and metamorphism beneath the Colorado Plateau. *Contrib. Mineral. Petrol.* **151**, 313–330.

Crowley J. L., Schoene B. and Bowring S. A. (2007) U–Pb dating of zircon in the Bishop Tuff at the millennial scale. *Geology* **35**, 1123–1126.

Davydov V. I., Crowley J. L., Schmitz M. D. and Poletaev V. I. (2010) High-precision U–Pb zircon age calibration of the global Carboniferous time scale and Milankovitch band cyclicity in the Donets Basin, eastern Ukraine. *Geochem. Geophys. Geosyst.* **11**, Q0AA04.

Geisler T. and Schleicher H. (2000) Improved U–Th–total Pb dating of zircons by electron microprobe using a simple new background modeling procedure and Ca as a chemical criterion of fluid-induced U–Th–Pb discordance in zircon. *Chem. Geol.* **163**, 269–285.

Geisler T., Pidgeon R. T., Kurtz R., van Bronswijk W. and Schleicher H. (2003) Experimental hydrothermal alteration of partially metamict zircon. *Am. Mineral.* **88**, 1496–1513.

Gerstenberger H. and Haase G. (1997) A highly effective emitter substance for mass spectrometric Pb isotope ratio determinations. *Chem. Geol.* **136**, 309–312.

Greenough J. D. and Dostal J. (1992) Cooling history and differentiation of a thick North Mountain Basalt flow (Nova Scotia, Canada). *Bull. Volcanol.* **55**, 63–73.

Griffin W. L. et al. (2002) Zircon chemistry and magma mixing, SE China: in-situ analysis of Hf isotopes, Tonglu and Pingtan igneous complexes. *Lithos* **61**, 237–269.

Hanchar J. M. and Miller C. F. (1993) Zircon zonation patterns as revealed by cathodoluminescence and backscattered electron images: implications for interpretation of complex crustal histories. *Chem. Geol.* **110**, 1–13.

Hanchar J. M. and van Westrenen W. (2007) Rare earth element behavior in zircon–melt systems. *Elements* **3**, 37–42.

Hanchar J. M. et al. (2001) Rare earth elements in synthetic zircon: Part 1. Synthesis, and rare earth element and phosphorus doping. *Am. Mineral.* **86**, 667–680.

Harley S. L., Kelly N. M. and Möller A. (2007) Zircon behaviour and the thermal history of mountain belts. *Elements* **3**, 25–30.

Hawkins D. P. and Bowring S. A. (1997) U–Pb systematics of monazite and xenotime: case studies from the Paleoproterozoic of the Grand Canyon, Arizona. *Contrib. Mineral. Petrol.* **127**, 87–103.

Hayden L. A. and Watson E. B. (2007) Rutile saturation in hydrous siliceous melts and its bearing on Ti-thermometry of quartz and zircon. *Earth Planet. Sci. Lett.* **258**, 561–568.

Hinton R. W. and Upton B. G. J. (1991) The chemistry of zircon: variations within and between large crystals from syenite and alkali basalt xenoliths. *Geochim. Cosmochim. Acta* **55**, 3287–3302.

Hofmann A., Valley J., Watson E., Cavosie A. and Eiler J. (2009) Sub-micron scale distributions of trace elements in zircon. *Contrib. Mineral. Petrol.* **158**, 317–335.

Hoskin P. W. O. and Ireland T. R. (2000) Rare earth element chemistry of zircon and its use as a provenance indicator. *Geology* **28**, 627–630.

Hoskin P. W. O. and Schaltegger U. (2003) The composition of zircon and igneous and metamorphic petrogenesis. *Rev. Mineral. Geochem.* **53**, 27–62.

Hoskin P. W. O., Kinny P. D., Wyborn D. and Chappell B. W. (2000) Identifying accessory mineral saturation during differentiation in granitoid magmas: an integrated approach. *J. Petrol.* **41**, 1365–1396.

Jaffey A. H., Flynn K. F., Glendenin L. E., Bentley W. C. and Essling A. M. (1971) Precision measurement of half-lives and specific activities of 235U and 238U. *Phys. Rev.* **C4**, 1889–1906.

Kelly N. M. and Harley S. L. (2005) An integrated microtextural and chemical approach to zircon geochronology: refining the Archaean history of the napier Complex, east Antarctica. *Contrib. Mineral. Petrol.* **149**, 57–84.

Krogh T. E. (1973) A low contamination method for hydrothermal decomposition of zircon and extraction of U and Pb for isotopic age determination. *Geochim. Cosmochim. Acta* **37**, 485–494.

Luo Y. and Ayers J. C. (2009) Experimental measurements of zircon/melt trace-element partition coefficients. *Geochim. Cosmochim. Acta* **73**, 3656–3679.

Macdonald F. A., Schmitz M. D., Crowley J. L., Roots C. F., Jones D. S., Maloof A. C., Strauss J. V., Cohen P. A., Johnston D. T. and Schrag D. P. (2010) Calibrating the cryogenian. *Science* **327**, 1241–1243.

Mattinson J. M. (2005) Zircon U–Pb chemical-abrasion ("CA-TIMS") method: combined annealing and multi-step dissolution analysis for improved precision and accuracy of zircon ages. *Chem. Geol.* **220**, 47–56.

Matzel J. P., Bowring S. A. and Miller R. B. (2006) Timescales of pluton construction at differing crustal levels: examples from the Mount Stuart and Tenpeak intrusions, North Cascades, WA. *GSA Bull.* **118**, 1412–1430.

Miller J. S. and Wooden J. L. (2004) Residence, resorption and recycling of zircons in Devils Kitchen Rhyolite, Coso Volcanic Field, California. *J. Petrol.* **45**, 2155–2170.

Miller J. S., Matzel J. P., Miller C. F., Burgess S. D. and Miller R. B. (2007) Zircon growth and recycling during the assembly of large, composite arc plutons. *Jour. Vol. Geotherm. Res.* **167**, 282–299.

Müller W. (2003) Strengthening the link between geochronology, textures and petrology. *Earth Planet. Sci. Lett.* **206**, 237–251.

Mundil R., Ludwig K. R., Metcalfe I. and Renne P. R. (2004) Age and timing of the Permian mass extinctions: U/Pb dating of closed-system zircons. *Science* **305**, 1760–1763.

Parrish R. R. (1990) U–Pb dating of monazite and its application to geological problems. *Can. J. Earth Sci.* **27**, 1431–1450.

Parrish R. R. and Noble S. R. (2003) Zircon U–Th–Pb geochronology by isotope dilution—thermal ionization mass spectrometry (ID-TIMS). In *Zircon*, vol. 53 (eds. J. M. Hanchar and P. W. O. Hoskin). Mineralogical Society of America, Washington, DC, pp. 183–213.

Prowatke S. and Klemme S. (2005) Effect of melt composition on the partitioning of trace elements between titanite and silicate melt. *Geochim. Cosmochim. Acta* **69**, 695–709.

Ramezani J. et al. (2007) High-precision U–Pb zircon age constraints on the Carboniferous–Permian boundary in the southern Urals stratotype. *Earth Planet. Sci. Lett.* **256**, 244–257.

Reid M. R., Coath C. D., Harrison T. M. and McKeegan K. M. (1997) Prolonged residence times for the youngest rhyolites associated with Long Valley caldera: ion microprobe dating of young zircons. *Earth Planet. Sci. Lett.* **150**, 27–38.

Reid M., Vazquez J. and Schmitt A. (in press) Zircon-scale insights into the history of a Supervolcano, Bishop Tuff, Long Valley, California, with implications for the Ti-in-zircon geothermometer. *Contrib. Mineral. Petrol.*

Rowley D. B., Xue F., Tucker R. D., Peng Z. X., Baker J. and Davis A. (1997) Ages of ultrahigh pressure metamorphism and protolith orthogneisses from the eastern Dabie Shan: U/Pb zircon geochronology. *Earth Planet. Sci. Lett.* **151**, 191–203.

Rubatto D. (2002) Zircon trace element geochemistry: partitioning with garnet and the link between U–Pb ages and metamorphism. *Chem. Geol.* **184**, 123–138.

Rubatto D. and Hermann J. (2007) Experimental zircon/melt and zircon/garnet trace element partitioning and implications for the geochronology of crustal rocks. *Chem. Geol.* **241**, 38–61.

Sano Y., Terada K. and Fukuoka T. (2002) High mass resolution ion microprobe analysis of rare earth elements in silicate glass, apatite and zircon: lack of matrix dependency. *Chem. Geol.* **184**, 217–230.

Schaltegger U., Fanning C. M., Günther D., Maurin J. C., Schulmann K. and Gebauer D. (1999) Growth, annealing and recrystallization of zircon and preservation of monazite in high-grade metamorphism: conventional and in-situ U–Pb isotope, cathodoluminescence and microchemical evidence. *Contrib. Mineral. Petrol.* **134**, 186–201.

Schaltegger U., Brack P., Ovtcharova M., Peytcheva I., Schoene B., Stracke A. and Bargossi G. (2009) Zircon and titanite recording 1.5 million years of magma accretion, crystallization and initial cooling in a composite pluton (southern Adamello batholith, northern Italy). *Earth Planet. Sci. Lett.* **286**, 108–218.

Schmitz M. D. and Schoene B. (2007) Derivation of isotope ratios, errors, and error correlations for U–Pb geochronology using ^{205}Pb–^{235}U–(^{233}U)-spike isotope dilution thermal ionization mass spectrometric data. *Geochem. Geophys. Geosyst.* **8**, Q08006.

Schoene B. and Bowring S. A. (2007) Determining accurate temperature–time paths in U–Pb thermochronology: an example from the SE Kaapvaal craton, southern Africa. *Geochim. Cosmochim. Acta* **71**, 165–185.

Schoene B., Crowley J. L., Condon D. C., Schmitz M. D. and Bowring S. A. (2006) Reassessing the uranium decay constants for geochronology using ID-TIMS U–Pb data. *Geochim. Cosmochim. Acta* **70**, 426–445.

Schoene B., Guex J., Bartolini A., Schaltegger U. and Blackburn T. J. (2010) Correlating the end-Triassic mass extinction and flood basalt volcanism at the 100,000-year level. *Geology* **38**, 387–390.

Simon J. I. and Reid M. R. (2005) The pace of rhyolite differentiation and storage in an 'archetypical' silicic magma system, Long Valley, California. *Earth Planet. Sci. Lett.* **235**, 123–140.

Slama J. et al. (2008) Plesovice zircon—a new natural reference material for U–Pb and Hf isotopic microanalysis. *Chem. Geol.* **249**, 1–35.

Sun S. S. and McDonough W. F. (1989) Chemical and isotopic systematics of oceanic basalts: implications for mantle composition and processes. *Geol. Soc. Lond. Spec. Publ.* **42**, 313–345.

Tepley F. J., Lundstrom C. C., Gill J. B. and Williams R. W. (2006) U–Th–Ra disequilibria and the time scale of fluid transfer and

andesite differentiation at Arenal volcano, Costa Rica (1968–2003). *J. Volcanol. Geotherm. Res.* **157**, 147–165.

Thomas J. B., Bodnar R. J., Shimizu N. and Sinha A. K. (2002) Determination of zircon/melt trace element partition coefficients from SIMS analysis of melt inclusions in zircon. *Geochim. Cosmochim. Acta* **66**, 2887–2901.

Tomaschek F., Kennedy A. K., Villa I. M., Lagos M. and Ballhaus C. (2003) Zircons from Syros, Cyclades, Greece—recrystallization and mobilization of zircon during high-pressure metamorphism. *J. Petrol.* **44**, 1977–2002.

Turner S., Bourdon B. and Gill J. (2003) Insights into magma genesis at convergent margins from U-series isotopes. *Rev. Mineral. Geochem.* **52**, 255–315.

Vavra G., Gebauer D., Schmid R. and Compston W. (1996) Multiple zircon growth and recrystallization during polyphase Late Carboniferous to Triassic metamorphism in granulites of the Ivrea Zone (Southern Alps): and ion microprobe (SHRIMP) study. *Contrib. Mineral. Petrol.* **122**, 337–358.

Vavra G., Schmid R. and Gabauer D. (1999) Internal morphology, habit and U–Th–Pb microanalysis of amphibolite-to-granulite facies zircons: geochronology of the Ivrea Zone (Southern Alps). *Contrib. Mineral. Petrol.* **134**, 380–404.

Wasserburg G. J., Jacousen S. B., DePaolo D. J., McCulloch M. T. and Wen T. (1981) Precise determinations of Sm/Nd ratios, Sm and Nd isotopic abundances in standard solutions. *Geochim. Cosmochim. Acta* **45**, 2311–2323.

Watson E. B. (1980) Some experimentally determined zircon/liquid partition coefficients for the rare earth elements. *Geochim. Cosmochim. Acta* **44**, 895–897.

Watson E., Wark D. and Thomas J. (2007) Crystallization thermometers for zircon and rutile. *Contrib. Mineral. Petrol.* **151**, 413–433.

Whitehouse M. J. and Kamber B. S. (2002) On the overabundance of light rare earth elements in terrestrial zircons and its implication for Earth's earliest magmatic differentiation. *Earth Planet. Sci. Lett.* **204**, 333–346.

Wilde S. A., Valley J. W., Peck W. H. and Graham C. M. (2001) Evidence from detrital zircons for the existence of continental crust and oceans on the Earth 4.4 Gyr ago. *Nature* **409**, 175–178.

Yuan H.-L., Gao S., Dai M.-N., Zong C.-L., Günther D., Fontaine G. H., Liu X.-M. and Diwu C. (2008) Simultaneous determinations of U–Pb age, Hf isotopes and trace element compositions of zircon by excimer laser-ablation quadrupole and multiple-collector ICP-MS. *Chem. Geol.* **247**, 100–118.

Associate editor: Yuri Amelin